

THE FATE OF NITROGEN DURING CORE-MANTLE SEPARATION D. S. Grewal¹ (dsg10@rice.edu), R. Dasgupta¹, A. K. Holmes¹, G. Costin¹, Y. Li^{1,2}, K. Tsuno¹. ¹Department of Earth, Environmental, and Planetary Sciences, Rice University, 6100 Main Street, MS 126, Houston, TX 77005, USA. ²Guangzhou Institute of Geochemistry, Chinese Academy of Sciences, Guangzhou, 510460, China.

Introduction: Nitrogen (N), the most dominant constituent of Earth's atmosphere, is critical for the habitability and existence of life on our planet. However, its distribution between Earth's major reservoirs, which must be largely influenced by the accretion and differentiation processes during its formative years, is poorly known. Sequestration into the metallic core, along with volatility-related loss pre- and post-accretion, could be a critical process that can explain the depletion of N in the Bulk Silicate Earth (BSE) relative to the primitive chondrites [1-2]. However, the relative effect of different thermodynamic parameters on the alloy-silicate partitioning behavior of N is still poorly known. Here we present equilibrium partitioning data of N between alloy and silicate melt ($D_N^{\text{alloy/silicate}}$) from 67 new high pressure ($P=1-6$ GPa)-temperature ($T=1500-2200$ °C) experiments under graphite saturated conditions at a wide range of oxygen fugacity ($\log fO_2$ ΔIW -4.2 to -0.8 , where IW refers to the fO_2 of the iron-wüstite buffer), mafic to ultramafic silicate melt compositions (NBO/T=0.4 to 2.2), and varying chemical composition of the alloy melts (S and Si contents of 0-32.1 wt.% and 0-3.1 wt.%, respectively).

Methods: The experiments were performed using piston cylinder and multi-anvil devices with alloy-silicate mixtures containing ~30-35 wt.% alloy and 65-70% wt.% silicate in graphite capsules. Combinations of 11 different alloy mixes and 7 different silicate mixes were used to simulate the redox conditions of Magma Oceans (MOs) as well as to test the compositional space for alloy and silicate systems applicable for an assortment of rocky bodies in the Solar System. Fe_4N/Fe_7N_3 were used as the N source under relatively oxidized conditions ($> \Delta IW -1.5$), while Si_3N_4 was the N source under reducing conditions ($< \Delta IW -1.5$).

The abundances of major and minor elements as well as N contents of the quenched experimental alloy and silicate melts were determined using a JEOL JXA8530F Hyperprobe EPMA at Rice University. LDE2 crystal was used to determine N abundances in the alloy and silicate phases using Fe_3N and BN standards, respectively.

Results: All experiments produced quenched metal blobs in silicate glass pools, except for experiments with more mafic silicate starting material, which produced quenched dendritic crystals in silicate melts. No

bubbles were observed in the quenched alloy and silicate products in any of the experiments, i.e., there was no N exsolution during quenching.

N partitioning between alloy and silicate melt

1) Effect of fO_2 :

To constrain the effect of fO_2 on $D_N^{\text{alloy/silicate}}$, we have plotted experiments from this study and other previous studies [3-4] at 1-7 GPa and 1600-1800 °C for S-free systems (Fig. 1). In accordance with results of [4], $D_N^{\text{alloy/silicate}}$ drops exponentially with decrease in $\log fO_2$ because the N content in the alloy melts decreases, while the N content in the silicate melts increases with decrease in $\log fO_2$. Additionally, at extremely reduced conditions ($< \Delta IW -3.0$), there is an extra drop in $D_N^{\text{alloy/silicate}}$, in addition to the $\log fO_2$ trend, at a given T , which can be explained by the incorporation of Si in the alloy melt.

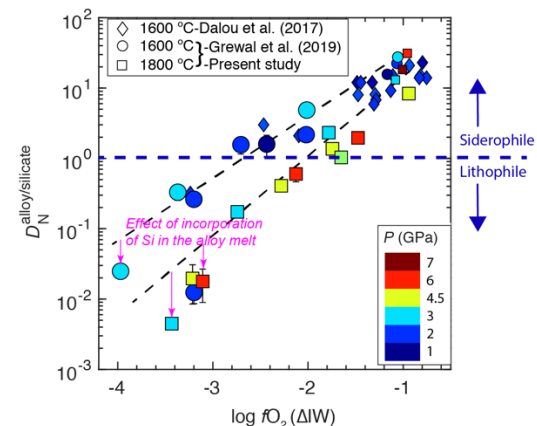


Fig. 1: $D_N^{\text{alloy/silicate}}$ as a function $\log fO_2$ at 1-7 GPa and 1600-1800 °C.

2) Effect of Temperature:

At a given fO_2 , $D_N^{\text{alloy/silicate}}$ decreases with increase in T because the N content in the alloy melt decreases, while the N content in the silicate melt increases with increase in T at a fixed fO_2 (Fig. 1). Furthermore, the negative effect of T on $D_N^{\text{alloy/silicate}}$ increases at increasingly reduced conditions.

3) Effect of S content in the alloy melt:

In agreement with [3], we found that at any given P - T in a relatively oxidized range ($\Delta IW -1.2$ to -0.7),

$D_{\text{N}}^{\text{alloy/silicate}}$ increases slightly from S-free alloy melt-bearing system to a system with ~16 wt.% S in the alloy melt, and it drops by a factor of two for a system with > ~20 wt.% S in the alloy melt (Fig. 2).

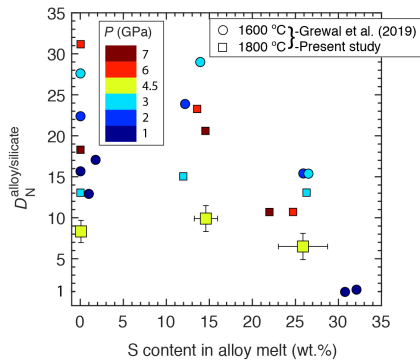


Fig. 2: $D_{\text{N}}^{\text{alloy/silicate}}$ as a function S content in the alloy melt at 1-7 GPa and 1600-1800 °C under relatively oxidizing conditions ($\Delta\text{IW} = 1.2$ to -0.7).

4) Effect of Pressure:

For the most oxidized experiments where N acts as a siderophile element, $D_{\text{N}}^{\text{alloy/silicate}}$ increases with increase in P from 1 to 3 GPa, then drops at 4.5 GPa followed by an increase at $P > 4.5$ GPa (Fig. 2). While at increasingly reducing conditions when N acts as a lithophile element, $D_{\text{N}}^{\text{alloy/silicate}}$ does not show any clear correlation with P (Fig. 1).

Discussion: Our multivariable parameterization for $D_{\text{N}}^{\text{alloy/silicate}}$, using experimental data from this study and several previous studies [3-10], shows that oxygen fugacity of the accreting material, along with Si content of the equilibrating alloy under extremely reducing conditions, followed by the temperature of alloy-silicate equilibration are the thermodynamic variables that primarily control nitrogen content in the residual MO for core formation scenarios applicable for a variety of rocky bodies in the Solar System.

Using parametrized $D_{\text{N}}^{\text{alloy/silicate}}$ for multi-stage core formation models applicable for Earth (Fig. 3), we predict that if Earth's accreting material had an FeO content similar to that of the present-day Earth's upper mantle (~8 wt.% FeO) 'Path 1' or evolved from relatively oxidized to present-day values with minimal incorporation of Si into the equilibrating alloy 'Path 2', then ~100 ppm bulk accreted N can satisfy the present-day BSE budget of N with minimal loss of N to space. However, if the proto-Earth initially accreted material that was much more reduced before evolving to the present-day FeO contents in the upper mantle

'Path 3', then during the initial stages of alloy-silicate equilibration, when significant amount of Si enters into the equilibrating alloy as well as due to extremely reduced state of silicate MO, almost all of the accreted N is retained in the MO.

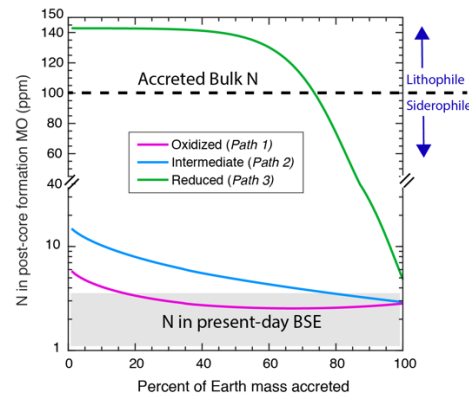


Fig. 3: Modelled N concentration in the post-core formation magma ocean as a function of the percentage of Earth mass accreted for three end-member accretion scenarios for a bulk N content of 100 ppm and assuming complete alloy-silicate equilibration.

For such scenarios, final stages of very efficient alloy-silicate equilibration with effectively Si free alloys is necessary to scavenge large amounts of N from the MO provided Earth's accreted bulk N budget was 100 ppm. If alloy-silicate equilibration was inefficient during the final stages of accretion and/or late stage core forming alloys had significant amounts of Si, then such scenarios demand that Earth's accreting material should either be extremely N-poor or large amounts of N have to be lost to space if Earth accreted material that was relatively N-rich. Therefore, if the late stage accretion of relatively large planetary embryo(s) (>0.01 ME) proceeded with inefficient equilibration of planetary embryo's core with proto-Earth's mantle and the bulk silicate portion of planetary embryo(s) was N-bearing, then the proto-Earth's mantle has to be N-poor or N-free owing to high degree of N loss to space prior to the accretion of planetary embryo(s).

References: [1] Marty B. (2012) *EPSL*, 313, 56–66. [2] Halliday A.N. (2013) *GCA*, 105, 146-171. [3] Grewal D. S. et al. (2019) *Sci. Adv.*, 5, eaau3669 [4] Dalou C. et al. (2017) *EPSL*, 458, 141-151. [5] Roskosz M. et al. (2013) *GCA*, 121, 15-28. [6] Li Y. et al. (2016) *GPL*, 138-147. [7] Kadik A. A. et al. (2011) *Geochem. Int.*, 49, 429-438. [8] Kadik A. A. et al. (2013) *PEPI*, 214, 14-24. [9] Kadik A. A. et al. (2015) *Geochem. Int.*, 53, 849-868. [10] Kadik A. A. et al. (2017) *Geochem. Int.*, 55, 151-162.